



**HAL**  
open science

# Handling large model uncertainty in adaptive feedback noise attenuation by overparametrization

Gabriel Buche, Bernard Vau, Ioan Doré Landau, Raul Melendez

► **To cite this version:**

Gabriel Buche, Bernard Vau, Ioan Doré Landau, Raul Melendez. Handling large model uncertainty in adaptive feedback noise attenuation by overparametrization. 2020. hal-02959414v1

**HAL Id: hal-02959414**

**<https://hal.science/hal-02959414v1>**

Preprint submitted on 6 Oct 2020 (v1), last revised 1 May 2021 (v2)

**HAL** is a multi-disciplinary open access archive for the deposit and dissemination of scientific research documents, whether they are published or not. The documents may come from teaching and research institutions in France or abroad, or from public or private research centers.

L'archive ouverte pluridisciplinaire **HAL**, est destinée au dépôt et à la diffusion de documents scientifiques de niveau recherche, publiés ou non, émanant des établissements d'enseignement et de recherche français ou étrangers, des laboratoires publics ou privés.

# Handling large model uncertainty in adaptive feedback noise attenuation by overparametrization

Gabriel Buche<sup>a</sup>, Bernard Vau<sup>b</sup>, Ioan Doré Landau<sup>1a</sup>, Raul Melendez<sup>a</sup>

<sup>a</sup>Univ. Grenoble Alpes, CNRS, Grenoble INP, GIPSA-lab, 38000 Grenoble, France

<sup>b</sup>Ixblue, 94380 Bonneuil-sur-Marne, France

---

## Abstract

Adaptive feedback noise attenuation is a very efficient way for strongly attenuating multiple tonal and narrow band disturbances with unknown and time varying characteristics. These adaptive schemes implement the internal model principle for cancelling disturbances combined with the Youla Kucera parametrization which allows to directly tune the disturbance compensation filter without explicit identification of the model of the disturbance. The efficient use of these schemes requires a good knowledge of the model of the compensatory path which can be obtained by experimental system identification. However there are potential applications where the characteristics of the compensatory path may change significantly during operation and this may lead to the instability of the system. The paper addresses the problem of handling large plant model uncertainties by overparametrization of the adaptive disturbance compensation filter. A methodology for designing adaptive feedback noise cancelers in the presence of large model uncertainties is proposed. In addition of the overparametrization a specific design of the linear feedback controller has to be done in order to satisfy a frequency condition in the range of variations of the frequencies characteristics of the model of the compensatory path. The experimental validation of the design is done on a relevant active noise control test bench.

*Keywords:* active noise control, adaptive feedback compensation, Youla–Kučera parametrization, model uncertainties

---

## 1. Introduction

For the rejection of multiple narrow band noise disturbances with unknown and time-varying characteristics an adaptive feedback solution has shown to be very efficient. Using such a solution, the need of an extra measurement of an image of the disturbance is removed as well as the presence of the undesirable positive internal feedback occurring in most of the adaptive feedforward attenuation schemes.

The essence of the adaptive feedback approach is to use the internal model principle which requires for the asymptotic rejection of the disturbance the inclusion in the controller of the model

---

<sup>1</sup>Corresponding author: Ioan Doré Landau (ioan-dore.landau@gipsa-lab.grenoble-inp.fr)

of the disturbance and combine this with a Youla-Kucera parametrization of the controller allowing to adaptively tune the parameters of the controller without explicit identification of the model of the disturbance.

The basic diagram of such a system is shown in Fig 1. In addition of a central polynomial controller ( $R_o, S_o$ ) there is a  $Q$  filter (FIR) termed the Youla-Kucera filter. This filter has as input the signal  $w(t)$  which can be viewed as the output of a disturbance observer [? ]

The first use of this approach in active noise attenuation is presented in [? ]. A more recent

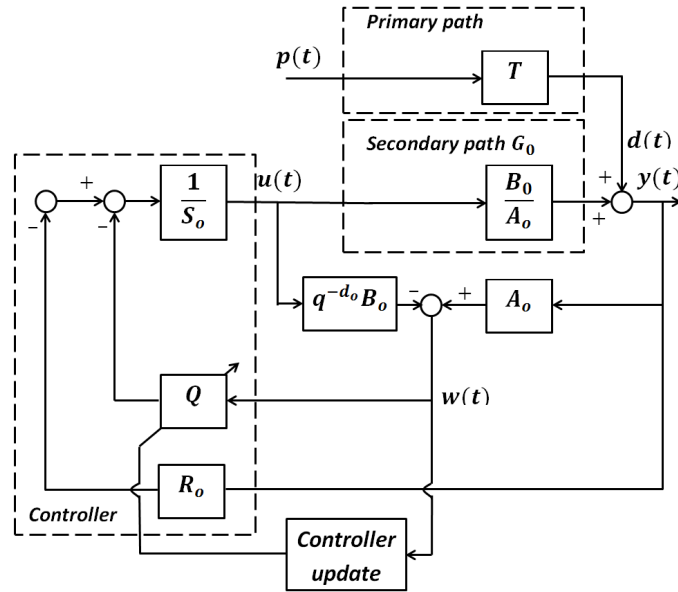


Figure 1: Youla-Kucera direct adaptive feedback regulation scheme.

application is [? ]. This approach has been extensively used in active vibration control [? ] and has been the subject of an international benchmark reported in a special issue of European Journal of Control [? ].

In this context it is assumed the the models of the narrow band noise disturbances are unknown but it is assumed that the model of the compensatory (secondary) path is known and almost constant. Excellent models of the compensatory path in active noise attenuation can be obtained by experimental system identification (very small differences between simulations and real experiments). See for example [? ? ]. Changes of the physical configurations and of various operational conditions lead to models of the same structure (with different orders and parameters). There are however potential applications in active noise attenuation where large variation of the model of the compensatory path may occurs and this will lead in most of the cases to instability of the system. So one of the crucial issues is how to take into account the plant model variations.

In [? ] where such an adaptive Youla-Kucera feedback scheme has been used for the rejection of an exponential type disturbance acting on a bio reactor characterized by a first order model, it was suggested that overparametrizing the adaptive  $Q$  filter is a possibility for handling not only the disturbance but also the uncertainties on the plant model. In [? ] it is argued that the robustness

of the scheme is enhanced by overparametrizing the Q filter and of course it should be possible to account for change in the plant models. In [?] an approach for rejecting unknown disturbances acting on an uncertain system using the dual Youla-Kucera parameterization [?] has been proposed. However no stability analysis is provided for the full scheme. In [?] the analysis of a scheme with an extended adaptive Q filter for the case of a first order system is provided. However these results can not be extended for systems of higher order like in active noise control where the orders of the plant models can be very high (often over 25).

The analysis of such an approach using overparametrization has been investigated in [?]. One of the basic finding is the fact that it is not enough to overparametrize the adaptive filter in order to guarantee the stability of the system. The system with overparametrized Q filter should do simultaneously two tasks: verify the internal model principle while guaranteeing the stability of the system. Even assuming that one knows the uncertainty, it results that there are a frequency condition for stability, In other terms this means that in addition of using overparametrization the controller has to be designed such that a frequency condition is satisfied for all the models in the set of possible models.

Furthermore, the fact that one uses overparametrization, the argument of richness of excitation of the disturbance can no longer be used for parameter convergence and stability analysis of the adaptive scheme. A specific analysis has to be done (this aspect has not been discussed in [?]). Since one uses overparametrization, the solution of the internal model principle is no more unique and different solutions may result for various initial conditions. However for stability reasons, the domain of possible values of the parameters should be bounded. Therefore the standard parameter adaptation algorithms have to be completed with a projection procedure to maintain the parameters within a certain domain of variations. For the case of unstructured uncertainties, this problem has been discussed in [?]. In the present paper such a procedure is proposed for the case of structured uncertainties and a stability analysis of the full scheme is provided.

A fundamental message which the paper tries to deliver is the following: A simple overparametrization of the adaptive Q filter is not enough for handling large plant uncertainties. An appropriate design of the linear controller has to be done and the basic adaptation algorithms have to be completed with a projection procedure.

The paper also shows that effectively this procedure for handling large model uncertainties can be implemented in adaptive feedback noise attenuation of multiple unknown narrow band disturbances and an experimental evaluation on a relevant test bench is provided.

The paper is organized as follows: In Section 2, the experimental setup will be described. In Section 3, the basic equations describing the system will be presented. Section 4 will present the methodology of designing the full system in order to handle plant model uncertainties. The experimental results obtained on the test bench are summarized in Section 6. Concluding remarks are presented in Section 7.

## **2. Experimental Setup**

The test bench allows to test active noise control in pipes for various physical configurations. The detailed scheme of the test bench with the control loop is shown in Fig. 2 and the views of

the two implementations which will be considered subsequently are shown in Fig. 3. The actual dimensions of the two implementations are given in Fig. 4

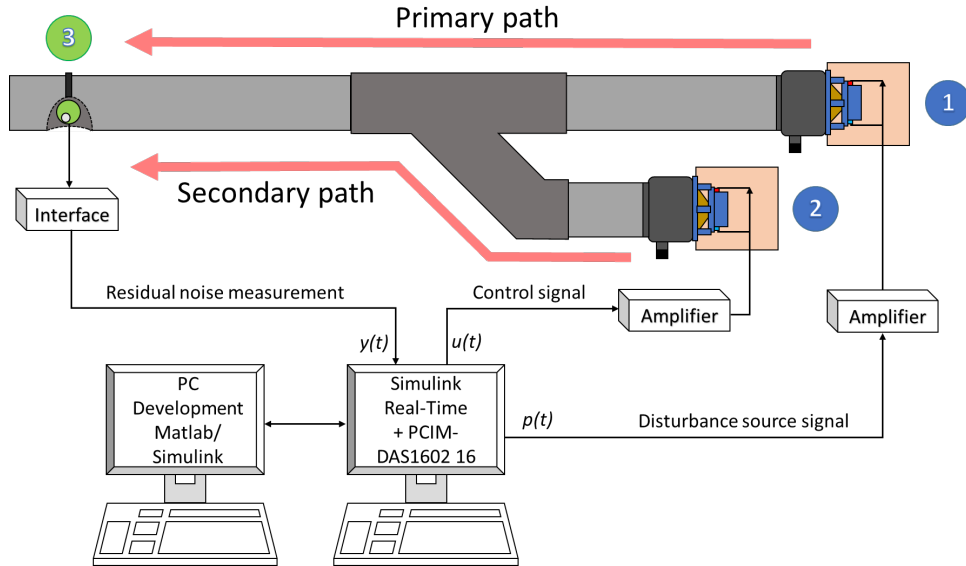


Figure 2: Duct active noise control test bench diagram.

In Fig. 2, the speaker used as the source of disturbances is labelled as 1, while the control speaker is marked as 2. At pipe's open end, the microphone that measures the system's output (residual noise) is denoted as 3. The control signal is denoted  $u(t)$ , the residual noise is denoted  $e(t)$ . The transfer function between the disturbance's speaker and the microphone (1→3) is called *Primary Path*, while the transfer function between the control speaker and the microphone (2→3) is denoted *Secondary Path*. These marked paths have a double differentiator behaviour, since as input we have the voice coil displacement and as output the air acoustic pressure.

Both speakers are connected to a xPC Target computer with Simulink Real-time<sup>®</sup> environment through a pair of high definition power amplifiers and a data acquisition board. A second computer is used for development, design and operation with Matlab<sup>®</sup>. The sampling frequency has been chosen in accordance with the recommendations given in [? ]. Taking into account that disturbances up to 400 Hz need to be attenuated, a sampling frequency  $f_s = 2500$  Hz has been chosen ( $T_s = 0.0004$  sec), i.e., approximately six times the maximum frequency to attenuate.

In this configuration, speakers are isolated inside wood boxes filled with special foam in order to create anechoic chambers and reduce the radiation noise produced. These boxes have dimensions  $0.15\text{ m} \times 0.15\text{ m} \times 0.12\text{ m}$ , giving a chamber volume of 2.7L.

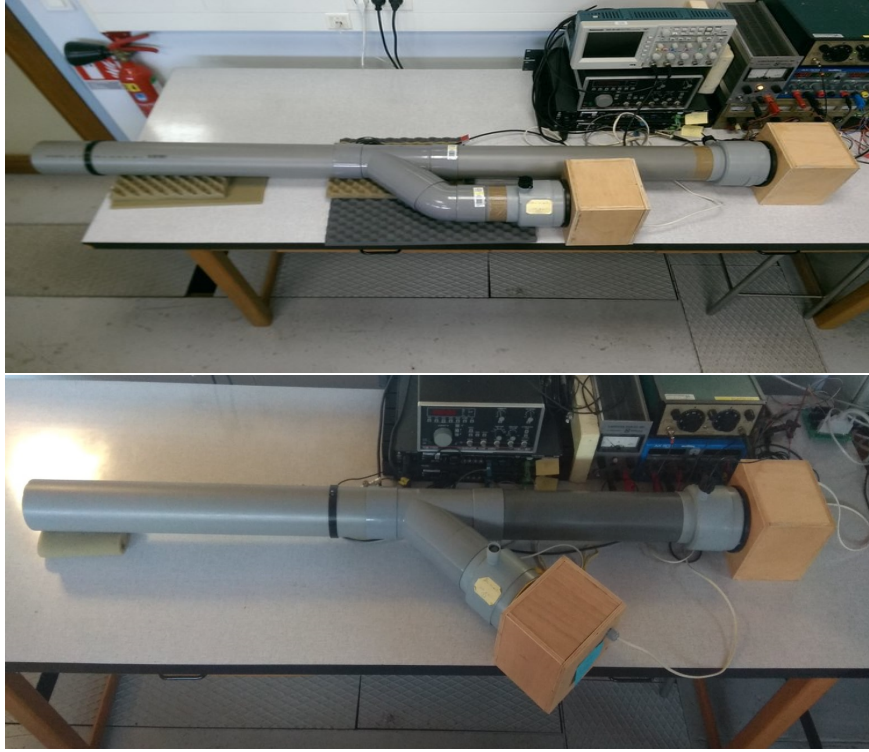


Figure 3: Duct active noise control test bench - Configuration Go (top), configuration G (bottom)

### 3. System structure

The model of the real plant<sup>2</sup> is denoted  $G(q^{-1})$  and is described by the transfer operator<sup>3</sup>:

$$G(q^{-1}) = \frac{q^{-d}B'(q^{-1})}{A(q^{-1})} = \frac{B(q^{-1})}{A(q^{-1})} \quad (1)$$

with:

$d$  = the plant pure time delay in number of sampling periods

$$\begin{aligned} A &= 1 + a_1q^{-1} + \dots + a_{n_A}q^{-n_A} ; \\ B' &= b_1q^{-1} + \dots + b_{n_B}q^{-n_B} = q^{-1}B^* ; \\ B'^* &= b_1 + \dots + b_{n_B}q^{-n_B+1} ; \\ B &= q^{-d}B'(q^{-1}) ; \\ B^* &= q^{-d}B'^*(q^{-1}) ; \end{aligned}$$

<sup>2</sup>In active vibration and noise control the plant is called "secondary path" or "compensation path"

<sup>3</sup>The complex variable  $z^{-1}$  will be used for characterizing the system's behavior in the frequency domain and the delay operator  $q^{-1}$  will be used for describing the system's behavior in the time domain.

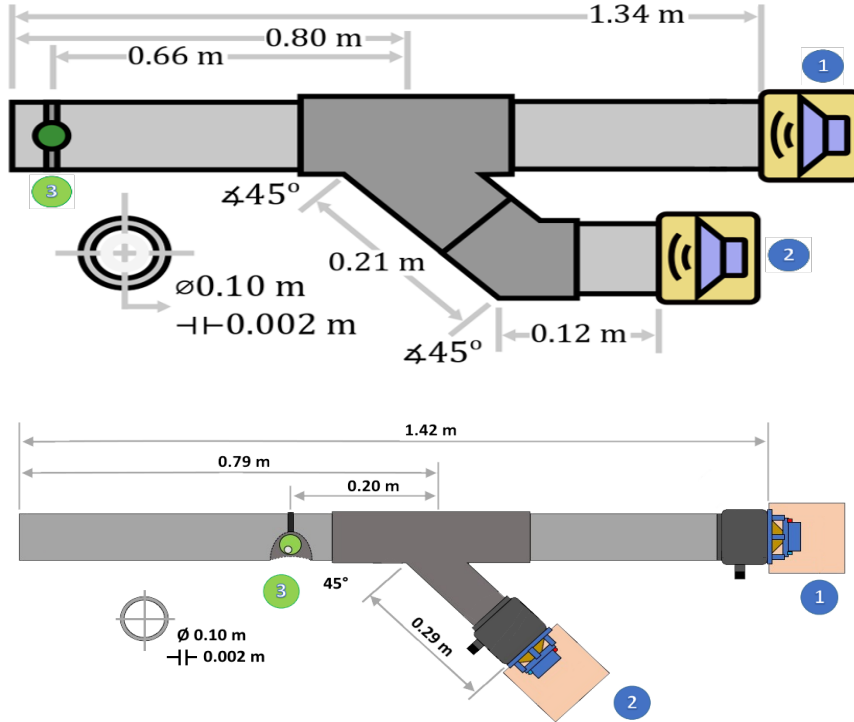


Figure 4: Duct active noise control test-bench dimensions - Go (top), G (bottom)

The plant model of the compensation path used for controller design (*design model*) is denoted  $G_o(q^{-1})$  and is described by:

$$G_o(q^{-1}) = \frac{q^{-d_o} B'_o(q^{-1})}{A_o(q^{-1})} = \frac{B_o(q^{-1})}{A_o(q^{-1})} \quad (3)$$

The secondary path models of the two configurations have been identified from experimental data using the methodology described in [? ]. Fig. 5 shows the frequency characteristics of the identified models. There are important differences between the two models. These characteristics present multiple resonances (low damped complex poles)<sup>4</sup> and anti-resonances (low damped complex zeros). The orders of the two models are summarized in Table 1. We will use the model of the secondary path of the configuration Go (design model) as the model for the design of a Youla-Kucera adaptive feedback noise attenuation scheme to be applied to the configuration G (real plant). The experiments will be carried on configuration G.

<sup>4</sup>The lowest damping is around 0.01.

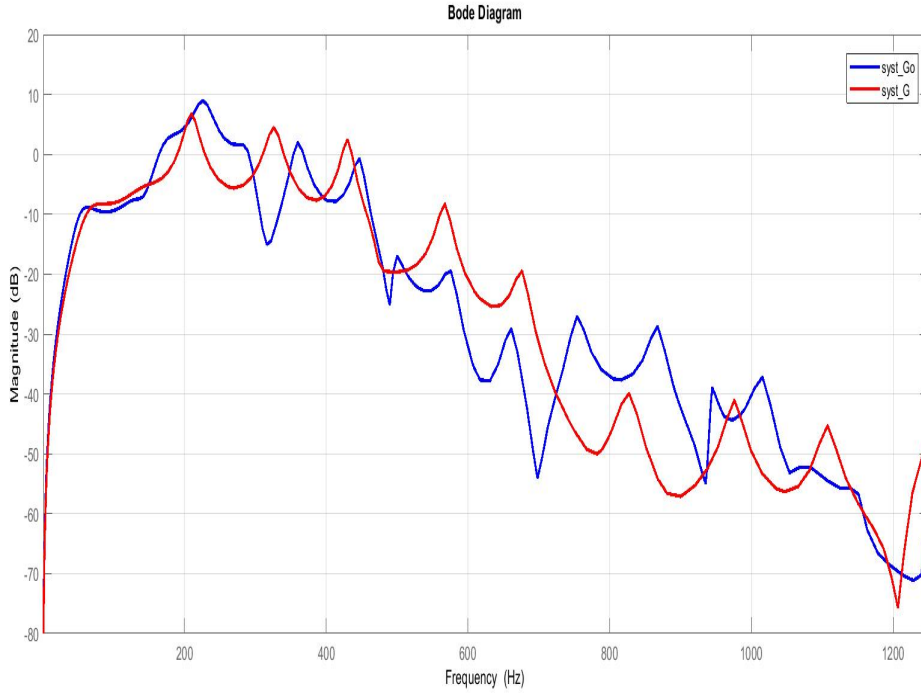


Figure 5: Bode diagrams of the nominal and uncertain plants

Model	$n_A$	$n_{B'}$	$d$
Secondary path $G_0$	38	32	8
Secondary path $G$	27	20	7

Table 1: Orders of the identified models.

## 4. Controller Design

### 4.1. Closed-loop structure

Let  $\{u(t)\}$ ,  $\{y(t)\}$ ,  $\{d(t)\}$  be respectively the control input, the system output, and the output disturbance sequences. The narrow band disturbance can be modelled as

$$d(t) = \frac{N_d(q^{-1})}{D_d(q^{-1})} \delta(t) \quad (4)$$

$\delta$  being the Dirac impulse, and where  $D_d(q^{-1})$  has its zeros on the unit circle. If the real plant model is equal to the design model, one has

$$y(t) = G_0(q^{-1})u(t) + d(t) \quad (5)$$

As shown in Fig. 1, the control structure is made of a disturbance observer providing an image  $w(t)$  of the disturbance, and a feedback structure yielding the signal  $u(t)$ . The disturbance observer is given by

$$w(t) = -B_0(q^{-1})u(t) + A_0(q^{-1})y(t) = A_0(q^{-1})d(t) \quad (6)$$

For the purpose of this paper the Q-filter of Fig. 1 is considered to be a polynomial of the form

$$Q(q^{-1}) = q_0^Q + q_1^Q q^{-1} + \dots + q_{n_Q}^Q q^{-n_Q} \quad (7)$$

In the general case, according to Fig. 1 a stabilizing R-S controller  $C_0$  is employed such that

$$C_0(q^{-1}) = \frac{R_0(q^{-1})}{S_0(q^{-1})} = \frac{R'_0(q^{-1})H_R(q^{-1})}{S'_0(q^{-1})H_S(q^{-1})} \quad (8)$$

where  $H_R(q^{-1})$  and  $H_S(q^{-1})$  are some fixed parts imposed during the controller synthesis. The polynomial defining the the poles of the feedback system in the absence of the Q filter is given by:

$$P_0(q^{-1}) = A_0(q^{-1})S_0(q^{-1}) + R_0(q^{-1})B_0(q^{-1}) \quad (9)$$

The Q-filter combined with the nominal controller leads to the controller  $C(q^{-1}) = \frac{R(q^{-1})}{S(q^{-1})}$  with

$$u(t) = -\frac{R(q^{-1})}{S(q^{-1})}y(t) \quad (10)$$

where

$$R(q^{-1}) = R_o + A_o H_R H_S Q \quad (11a)$$

$$S(q^{-1}) = S_o - B_o H_R H_S Q \quad (11b)$$

By simple computation, it can be shown that the poles of the closed loop remain unchanged in the case of a Q filter having the structure given in Eq. 7.

According to the internal model principle of Woonam [? ? ], in order to reject asymptotically the disturbance  $d(t)$ , the controller  $C$  must include in the polynomial  $S$  the denominator  $D_p$  of a model of the disturbance and owing to (4) and (11) one must have

$$S = S' D_d = S_o - H_R H_S B_o Q \quad (12)$$

and the optimal value of Q is obtained by solving the Bezout equation:

$$S' D_d + H_R H_S B_o Q = S_o \quad (13)$$

for  $D_d(q^{-1}) = 1 + d_1 q^{-1} + \dots + d_{n_D} q^{-n_D}$ . This Bezout equation (13) has a solution if  $D_d$  and  $H_R H_S q^{-d_o} B_o$  are coprime, and a minimal solution is obtained for  $n_Q = n_D - 1$ .

#### 4.1.1. The real plant differs with respect to the design model

In the general case the real plant  $G(q^{-1}) = \frac{B(q^{-1})}{A(q^{-1})}$  differs from  $G_0$ . Consequently, the scheme of Fig. 1 is modified: the true secondary path is now  $G$  instead of  $G_0$ , but the disturbance observer remains the one given by (6), and one has now

$$y(t) = G(q^{-1})u(t) + d(t) = \frac{B(q^{-1})}{A(q^{-1})}u(t) + d(t) \quad (14)$$

In a first step, we will analyze this configuration in order to see if assuming that the model of the disturbance is known one can find a polynomial  $Q$  which leads to a stable closed loop system and allows asymptotic rejection of the disturbance.

Different structures for the central controller can be considered. Since both  $G$  and  $G_o$  are asymptotically stable and in order to avoid the design of controller stabilizing both  $G$  and  $G_o$  one considers in the sequel a simplification to the controller structure by imposing  $R_0 = 0$  and  $H_S = 1$ . Therefore, from (10) and (11), the control signal becomes

$$u(t) = -\frac{R}{S} = -\frac{A_0 H_R Q}{S_0 - B_0 H_R Q} y(t) \quad (15)$$

To express the control  $u(t)$  as a function of  $w(t)$ , from Eq. (15) one obtains:

$$S_0 u(t) = -H_R Q (A_0 y(t) - B_0 u(t)) \quad (16)$$

from which it results using (6) :

$$u(t) = -\frac{H_R(q^{-1})}{S_0(q^{-1})} Q(q^{-1}) w(t) \quad (17)$$

This control structure corresponds to Fig. 6.

According to (14), the closed-loop polynomial including  $G$  and the simplified version of the controller is

$$P = AS_0 + QH_R(BA_0 - B_0A) \quad (18)$$

which must have all its roots strictly inside the unit circle. In this case ( $G \neq G_0$ ), the signal  $w(t)$  is expressed from  $d(t)$  according to

$$w(t) = \frac{AS_0A_0}{AS_0 + QH_R(BA_0 - B_0A)} d(t) \quad (19)$$

The derivation of this equation is given in Appendix A.

The output sensitivity function from  $d(t)$  to  $y(t)$  is given in this case by

$$y(t) = \frac{AS}{P} d(t) = \frac{A(S_0 - B_0 H_R Q)}{AS_0 + QH_R(BA_0 - AB_0)} d(t) \quad (20)$$

The derivation of this expression is given in Appendix B.

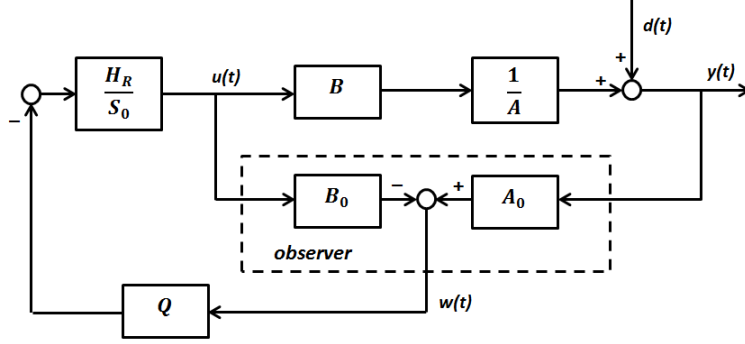


Figure 6: Linear controller structure for the case of known disturbances

In case of an uncertain plant a stability condition appears: The polynomial  $AS_0 + QH_R(BA_0 - B_0A)$  must have all its roots strictly inside the unit circle, and on the other hand the internal model condition (13) must be satisfied at the same time, in order to reject asymptotically  $d(t)$ . For a given order of the Q-filter, these two conditions may not be simultaneously met. In such a situation one can augment the order of  $Q(q^{-1})$ . Non-minimal solution to (13) can be parametrized as  $Q(q^{-1}) = \bar{Q}(q^{-1}) + V(q^{-1})D_D(q^{-1})$ , [?] and (13) becomes

$$\left(S' - VB_oH_RH_S\right)D_d + H_RH_SB_o(\bar{Q} + VD_d) = S_o \quad (21)$$

where  $V(q^{-1})$  is any polynomial (there is no need for it to be monic), and  $\bar{Q}$  the minimal solution of (13). The basic question is: does it exist a polynomial  $Q(q^{-1})$  with a degree  $n_Q < \infty$  satisfying (21) and guaranteeing the closed-loop stability.

Under the hypothesis that  $G_0, G$  are stable and that  $S_0$  has all its zeros strictly inside the unit circle, the sufficient conditions for the existence of a finite dimensional Q-filter which stabilizes the closed-loop and ensures the asymptotic rejection of the disturbance  $d(t)$  are:

- 1) At the frequencies  $\omega_j$  of the disturbance corresponding to  $D_d(e^{i\omega_j}) = 0$  one has

$$\left| \frac{B(e^{-i\omega_j})}{B_0(e^{-i\omega_j})} \frac{A_0(e^{-i\omega_j})}{A(e^{-i\omega_j})} - 1 \right| < 1 \quad (22)$$

- 2) At all other frequencies the following inequality is verified

$$|Q(e^{-i\omega})| < \left| \frac{A(e^{-i\omega})}{B(e^{-i\omega})A_0(e^{-i\omega}) - A(e^{-i\omega})B_0(e^{-i\omega})} \right| \left| \frac{S_0(e^{-i\omega})}{H_R(e^{-i\omega})} \right| \quad (23)$$

The derivation of conditions (22) and (23) is given in Appendix C.

From this analysis, one concludes that we have to satisfy two conditions. The first condition (22) depends only upon the discrepancy of the two models and defines the frequency zones where

asymptotic rejection of the disturbances can be achieved. The second condition indicates that one has to design  $S_0$  and  $H_r$  such the modulus of the right hand side of Eq. (23) is maximized in the frequencies regions outside the attenuation zone.

#### 4.2. Adaptive disturbance rejection

In the presence of unknown narrow band disturbances the polynomial  $D_d(q^{-1})$  is unknown. In this situation one can consider a Q-filter with adjustable parameters:

$$\hat{Q}(q^{-1}, t) = \hat{q}_0^Q(t) + \dots + \hat{q}_{n_Q}^Q(t)q^{-n_Q} \quad (24)$$

and the objective is to find a parameter adaptation algorithms driving these parameters towards the values assuring asymptotic rejection of the disturbance and assuring the stability of the system. We will follow up to certain extent the development procedure described in [?] however including from the beginning the presence of model uncertainties and the use of a Q filter of higher order than the minimal one used for the nominal case (when  $G = G_0$ ). From (19) one can express  $d(t)$  as a function of  $w(t)$  and plugging this expression in (20) one gets:

$$y(t) = \left( \frac{1}{A_0} - \hat{Q} \frac{H_R B_0}{A_0 S_0} \right) w(t) \quad (25)$$

where now the Q filter has been replaced by its estimation. The purpose of the control structure is to drive  $y(t)$  towards 0, and for this reason one defines an a-posteriori prediction error  $v(t+1)$  at time  $t+1$ , such that  $v(t+1) = y(t+1)$  thus

$$v(t+1) = \left( \frac{S_0}{A_0 S_0} - \hat{Q} \frac{H_R B_0}{A_0 S_0} \right) w(t+1) \quad (26)$$

But according the internal model principle the expression of  $Q$  that satisfies the internal model principle is given by (13), and by substituting in (26) one obtains

$$v(t+1) = (Q - \hat{Q}) \frac{H_R B_0}{A_0 S_0} w(t+1) + p(t+1) \quad (27)$$

where

$$p(t+1) = \frac{S' D_d}{A S_0 + Q H_r (B A_0 - B_0 A)} \cdot \frac{N_d}{D_d} \delta(t) \quad (28)$$

is a vanishing term assuming that the optimal Q stabilizes also the system.

One can define:

$$w_1(t) = \frac{1}{A_0} w(t) \quad (29a)$$

$$w_2(t) = \frac{B_0(q^{-1}) H_R(q^{-1})}{A_0(q^{-1}) S_0(q^{-1})} w(t+1) \quad (29b)$$

$$\hat{\mathbf{w}}^T(t) = [\hat{\mathbf{q}}_0^Q(t) \hat{\mathbf{q}}_1^Q(t) \dots \hat{\mathbf{q}}_{n_Q}^Q(t)] \quad (29c)$$

$$\mathbf{w}^T(t) = [\mathbf{q}_0^Q(t) \mathbf{q}_1^Q(t) \dots \mathbf{q}_{n_Q}^Q(t)] \quad (29d)$$

$$\mathbf{r}^T(t) = [w_2(t) w_2(t-1) \dots w_2(t-n_Q)] \quad (29e)$$

$$(29f)$$

The a-priori adaptation error is:

$$\mathbf{v}^\circ(t+1) = w_1(t+1) - \mathbf{r}^T(t)\hat{\mathbf{w}}(t) \quad (30)$$

and the a-posteriori adaptation error is given by:

$$\mathbf{v}(t+1) = \frac{\mathbf{v}^\circ(t+1)}{1 + \mathbf{r}^T(t)\mathbf{F}(t)\mathbf{r}(t)} \quad (31)$$

The a-posteriori adaptation error (27) can be expressed now under the form

$$\mathbf{v}(t+1) = H(q^{-1})(\mathbf{w} - \hat{\mathbf{w}}(t+1))^T \mathbf{r}(t) \quad (32)$$

where  $H(q^{-1}) = 1$ .

In order to estimate the coefficients of  $\hat{Q}(q^{-1}, t)$ , it is natural to use a Parameter Adaptation Algorithm (PAA). Taking into account the fact that the order of the polynomial  $\hat{Q}$  is higher than the minimal order required by the IMP, the parameter adaptation algorithm proposed in [?] has to be completed with a projection of the estimated parameter vector on a bounded domain in order to prove the stability of the adaptive control scheme (see [?] p.340). Based on stability considerations, a general form for the PAA has been proposed in [?] which can be expressed using the formalism of [?] as:

$$\hat{\mathbf{w}}(t+1) = \hat{\mathbf{w}}_p(t) + \mathbf{k}(t)\mathbf{v}(t+1) \quad (33)$$

$$\mathbf{v}(t+1) = \frac{\mathbf{v}^\circ(t+1)}{1 + \mathbf{r}^T(t)\mathbf{F}(t)\mathbf{r}(t)} \quad (34)$$

$$\mathbf{F}(t+1) = \frac{1}{\lambda_1(t)} \left[ \mathbf{F}(t) - \frac{\mathbf{F}(t)\mathbf{r}(t)\mathbf{r}^T(t)\mathbf{F}(t)}{\frac{\lambda_1(t)}{\lambda_2(t)} + \mathbf{r}^T(t)\mathbf{F}(t)\mathbf{r}(t)} \right] \quad (35)$$

$$1 \geq \lambda_1(t) > 0 \quad ; \quad 0 \leq \lambda_2(t) < 2 \quad ; \quad F(0) > 0 \quad (36)$$

where

$$\hat{\mathbf{w}}'(t) = F(t)^{-1/2}\hat{\mathbf{w}}(t) \quad (37a)$$

$$\hat{\mathbf{w}}'_p(t) = \hat{\mathbf{w}}'(t) \quad \text{if } \hat{\mathbf{w}}'(t) \in \mathcal{D}' \quad (37b)$$

$$\hat{\mathbf{w}}'_p(t) = \perp \text{proj of } \hat{\mathbf{w}}'(t) \text{ on } \mathcal{D}' \quad \text{if } \hat{\mathbf{w}}'(t) \notin \mathcal{D}' \quad (37c)$$

$$\hat{\mathbf{w}}_p(t) = F(t)^{1/2}\hat{\mathbf{w}}'_p(t) \quad (37d)$$

The projection domain  $\mathcal{D}'$  is defined as follows

$$\hat{\mathbf{w}} \in \mathcal{D}, \quad \hat{\mathbf{w}}'(t) = F(t)^{-1/2}\hat{\mathbf{w}}(t) \in \mathcal{D}' \quad (38)$$

where the projection domain  $\mathcal{D}$  is such that:

$$\mathcal{D} : \|\hat{\mathbf{w}}(t)\|_2^2 < \mathcal{R} < \infty \quad (39)$$

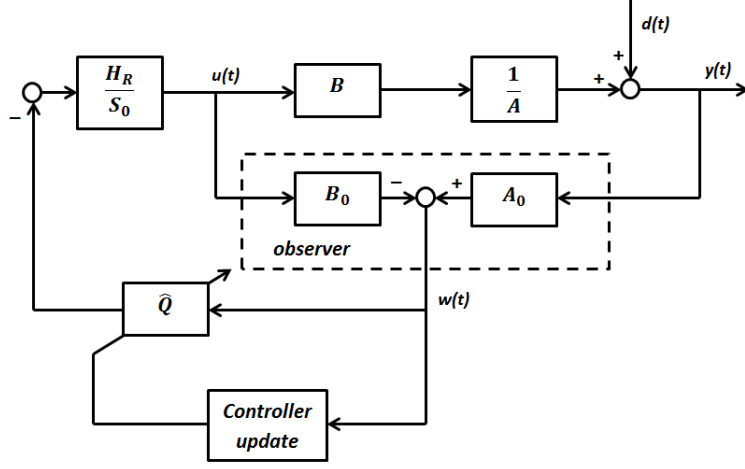


Figure 7: Adaptive control structure

The adaptive control structure is given in Fig. 7. The stability analysis of the full system is discussed in Appendix D.

Two particular choices for the adaptation gain are used mainly in practice in order to assure the alertness of the adaptation with respect to possible variations of the disturbance characteristics<sup>5</sup>:

- *Constant trace*- for a constant ratio  $\lambda_1(t)/\lambda_2(t)$ ,  $\lambda_1(t)$  is chosen such that the trace of the adaptation gain matrix  $F(t)$  remain constant ( $\text{trace } F(t) = \text{trace } F_0$ )
- *Constant gain*  $\lambda_1(t) = 1, \lambda_2(t) = 0$  and therefore  $F(t) = F_0$ <sup>6</sup>.

When using a constant adaptation gain, the change of coordinates introduced in Eqs. (37) and (38) is no more necessary (see [? ], pg.340-343) and Eqs (37) and (38) are replaced by:

$$\hat{\mathbf{w}}_p(t) = \hat{\mathbf{w}}(t) \quad \text{if } \hat{\mathbf{w}}(t) \in \mathcal{D} \quad (40)$$

$$\hat{\mathbf{w}}(t) = \perp \text{proj of } \mathbf{w}(t) \text{ on } \mathcal{D} \quad \text{if } \hat{\mathbf{w}}(t) \notin \mathcal{D} \quad (41)$$

This drastically simplifies the implementation of the algorithm. This simplification is also used for the case of a constant trace adaption gain (however in this case it is an approximation of the exact algorithm). In practice a bound on the parameters of the polynomial Q is fixed and when one of the parameters hits the bound, the algorithm is restarted with all the parameters at 0 ( i.e. one takes  $\hat{\mathbf{w}}_p(t) = 0$  in Eq. 33 (other options are also possible).

<sup>5</sup>For other options see [? ]

<sup>6</sup>In most of the cases one choose  $F_0 = gI, g > 0$ . This is known also as *constant scalar gain*

## 5. Tuning of the filter Hr/So

Firstly, it is necessary to check the frequency band for which a disturbance rejection is feasible, or in other words the frequency band where condition (22) is satisfied. For this purpose one plots  $\left| \frac{B(e^{-i\omega})A_0(e^{-i\omega})}{B_0(e^{-i\omega})A(e^{-i\omega})} - 1 \right|$  as a function of  $\omega$ . In the specific example of this paper, the corresponding graph is displayed in Fig. 8.

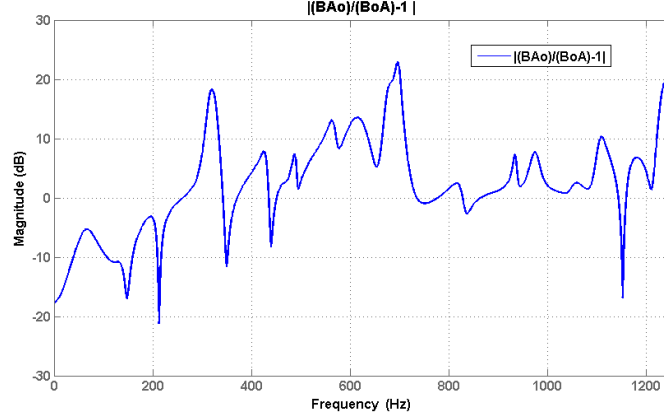


Figure 8: Magnitude of  $\frac{B(q^{-1})A_0(q^{-1})}{A(q^{-1})B_0(q^{-1})} - 1$

In this example, an adaptive rejection of the disturbance is feasible roughly up to 250 Hz. In order to design the filter  $\frac{H_R(q^{-1})}{S_0(q^{-1})}$ , it is useful to plot  $\left| \frac{A(e^{-i\omega})}{B(e^{-i\omega})A_0(e^{-i\omega}) - A(e^{-i\omega})B_0(e^{-i\omega})} \right|$ , see Fig. 9 (top).

In order to guarantee condition (23) for the largest possible family of Q filters, the product  $\left| \frac{A(e^{-i\omega})}{B(e^{-i\omega})A_0(e^{-i\omega}) - A(e^{-i\omega})B_0(e^{-i\omega})} \right| \left| \frac{S_0(e^{-i\omega})}{H_R(e^{-i\omega})} \right|$  must be maximized, and for this purpose the magnitude of  $\frac{S_0(q^{-1})}{H_R(q^{-1})}$  is increased as much as possible at the frequencies where the magnitude of  $\frac{A(q^{-1})}{B(q^{-1})A_0(q^{-1}) - A(q^{-1})B_0(q^{-1})}$  is low. A solution consists in choosing the filter  $\frac{H_R(q^{-1})}{S_0(q^{-1})}$  as a product of  $n_k$  second order filters:

$$\frac{H_R(q^{-1})}{S_0(q^{-1})} = \prod_{k=1}^{n_k} \frac{L_{Nk}(q^{-1})}{L_{Dk}(q^{-1})} \quad (42)$$

where each filter  $\frac{L_{Nk}(q^{-1})}{L_{Dk}(q^{-1})}$  results from the discretization of continuous resonating filter at the frequency  $\omega_k$  for  $k \leq n_k - 1$ :

$$\frac{\frac{s^2}{\omega_k^2} + 2\zeta_{Nk}s + 1}{\frac{s^2}{\omega_k^2} + 2\zeta_{Dk}s + 1}$$

with  $0 \leq \zeta_{Nk} < 1$ ,  $0 < \zeta_{Dk} \leq 1$  and  $\zeta_{Nk} < \zeta_{Dk}$ . Moreover, one of the filters  $\frac{L_{Nn_k}(q^{-1})}{L_{Dn_k}(q^{-1})}$  has two zeros at  $+1$  and  $-1$  and  $L_{Dn_k}(q^{-1}) = 1$  in order to open the loop at 0 Hz (the system has no gain at this

frequency and it is not reasonable to send a dc signal) and at the Nyquist frequency (for reducing the gain of the filter in high frequencies).

As a result, the magnitude of  $\frac{S_0(q^{-1})}{H_R(q^{-1})}$  is made of resonances at frequencies  $\omega_k$ . Fig. 9 (middle) displays the magnitude of this filter for this application. The first resonance frequency is equal to 225 Hz, and the magnitude of  $\frac{S_0(q^{-1})}{H_R(q^{-1})}$  for frequencies between 80 Hz and 210 Hz is left sufficiently low. For frequencies higher than 225 Hz a series of resonances guarantee that this magnitude is sufficiently high. Fig. 9 (bottom), presents the frequency characteristics of the right part of (23). One can see the effect of the filter  $H_R/S_0$ .

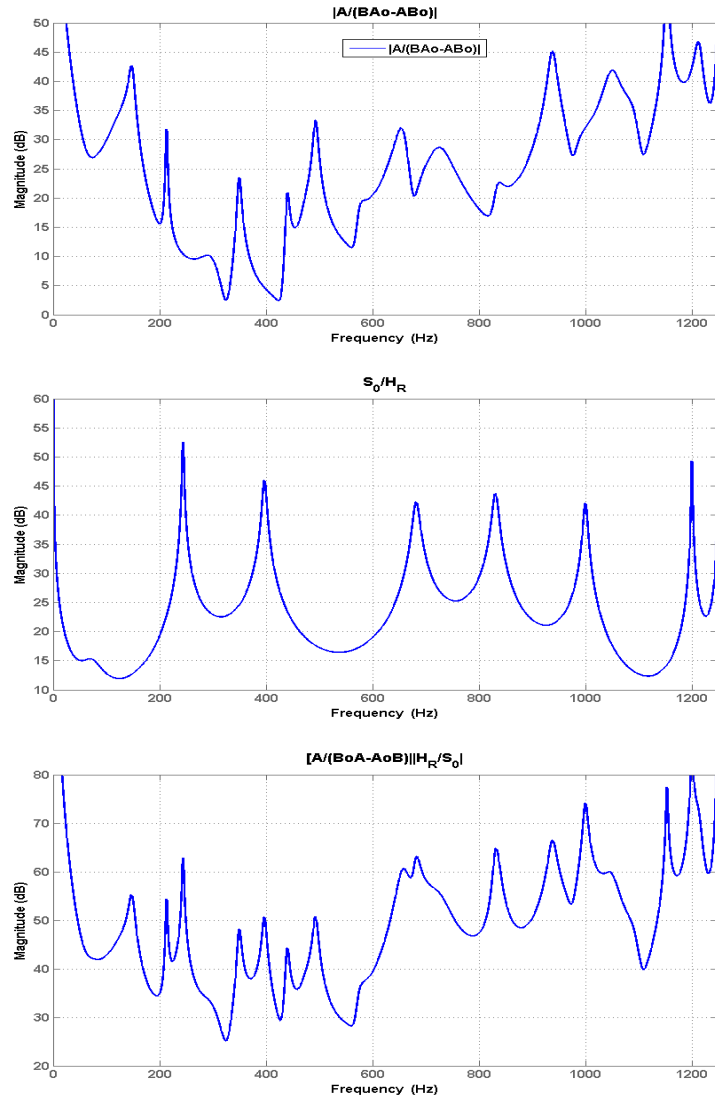


Figure 9: Magnitude of  $\frac{A(q^{-1})}{B(q^{-1})A_0(q^{-1})-A(q^{-1})B_0(q^{-1})}$  (Top), Magnitude for  $\frac{S_0(q^{-1})}{H_R(q^{-1})}$  (middle), Magnitude of  $\frac{A(q^{-1})}{B(q^{-1})A_0(q^{-1})-A(q^{-1})B_0(q^{-1})} \frac{S_0(q^{-1})}{H_R(q^{-1})}$  (bottom)

## 6. Experimental Results

The objective of the experimental validation is to assess the performance of the overparametrized YK adaptive feedback scheme on the configuration G using the the model of the configuration Go for implementing the YK observer (*uncertainty case*)

### 6.1. Performance on configuration G when using model Go

The performance will be evaluated using: 1) a single sinusoidal disturbance, 2) two sinusoidal disturbances with very close frequencies (*interference phenomenon*), 3) two sinusoidal disturbances with distinct frequencies. This evaluation will be done over the frequency range of operation. For all the experiments a constant trace adaptation gain is used.

#### 6.1.1. The case of a single sinusoidal disturbance

For the case of a single sinusoid it was found that using a Q filter with  $nQ = 15$  (16 parameters), good performance can be obtained over a range of operation between 80 Hz and 180 Hz. Use of  $nQ < 11$  (12 parameters) leads to instabilities for almost all the frequencies within this range. The attenuation in steady state<sup>7</sup> for various frequencies of the disturbance are summarized in row 2 of Table 2 . Fig. 10 shows the time response for the rejection of a single 160 Hz sinusoidal

Frequency (Hz)	70	80	120	160	180	190	210	220
Model Go, 16 par.(dB)	45.64	69.04	61.89	81.05	88.41	Oscil.	Oscil.	Oscil.
Model Go, 30 par.(dB)	67.02	74.84	74.84	77.98	90.92	90.44	77.71	76.42 .
Model Go, 60 par.(dB)	69.04	75.84	72.94	78.86	90.42	93.92	84.95	81.34 .

Table 2: Steady state attenuation for a single sinusoidal noise disturbance on configuration G

disturbance . The system operate in open loop for the first 5 s. Fig. 11 shows the power spectral density (PSD) of the residual noise in open loop and in closed loop for the same disturbance (the PSD is evaluated over an horizon of 3s). Fig. 12 shows the response of the residual noise for a sequence of step changes in the frequency of the disturbance around 160 Hz. The system operates in open loop for 5 s and then at  $t=50$  s a step of -10 Hz (150 Hz) is applied. Then the system returns to the nominal frequency at  $t=100$  s and at  $t=150$  s a step of +10 Hz (170 Hz) is applied. The corresponding evolution of the parameters is shown in Fig. 13. When using a Q filter with 16 parameters ( $nQ = 15$ ) oscillations occur for sinusoidal disturbances with frequencies equal or higher than 190 Hz. However augmenting the size of the Q filter to 30 parameters ( $nQ = 29$ ) one can go up to 220 Hz. The steady state attenuation for various frequencies of the disturbance for  $nQ = 29$  can be found in Table 2, row 3. Augmenting the size of the Q filter to  $nQ = 59$  (60 parameters) allows to improve the performance at the border of the operation region but does not allow to go to higher frequencies. The steady state attenuation for this case is summarized in Table 2, row 4.

<sup>7</sup>The attenuation is defined as the ratio between the variance of the residual noise in open loop and the variance of the residual noise in closed loop

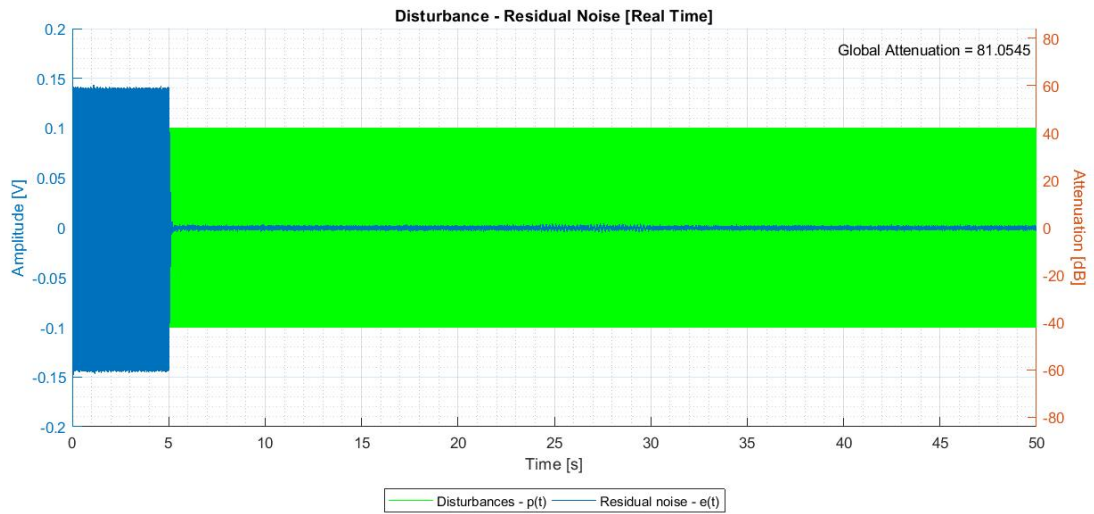


Figure 10: Evolution of the Residual noise for a 160 Hz sinusoidal disturbance (16 parameters).

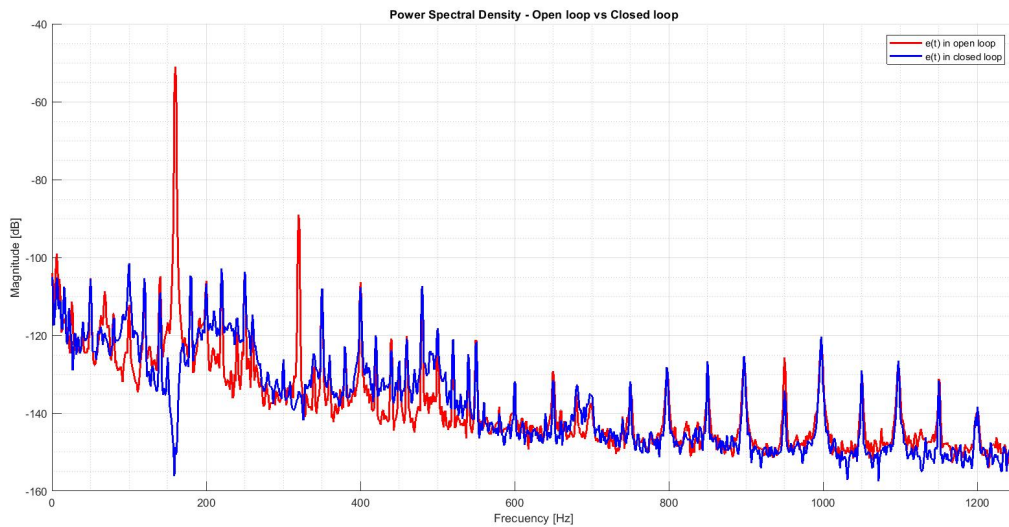


Figure 11: Power Spectral density of the residual noise in open loop and in closed loop for a 160 Hz sinusoidal disturbance (16 parameters) .

### 6.1.2. Adaptive attenuation of interferences

Fig. 14 shows the capability of the control scheme to strongly attenuate interference (interference occurs when two sinusoidal disturbances have very close frequencies). A couple of sinusoids at 140 Hz and 140.5 Hz is applied. Then at  $t=50$  s one switches to 130 Hz and 130.2 Hz, at  $t=100$  s one return to 140 Hz and 140.5 Hz and at  $t=150$  s one switches to 150 Hz and 150.3 Hz. The system operates in open loop for the first 5s. The corresponding evolution of the parameters (16 parameters) is shown in Fig. 15

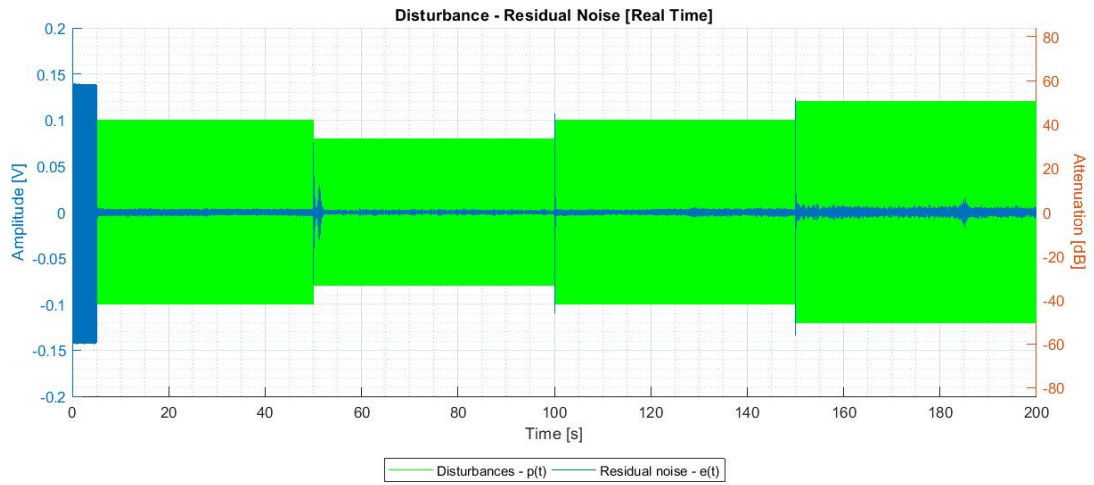


Figure 12: Time response of the residual noise for step changes in the frequency of the disturbance around 160 Hz (16 parameters)

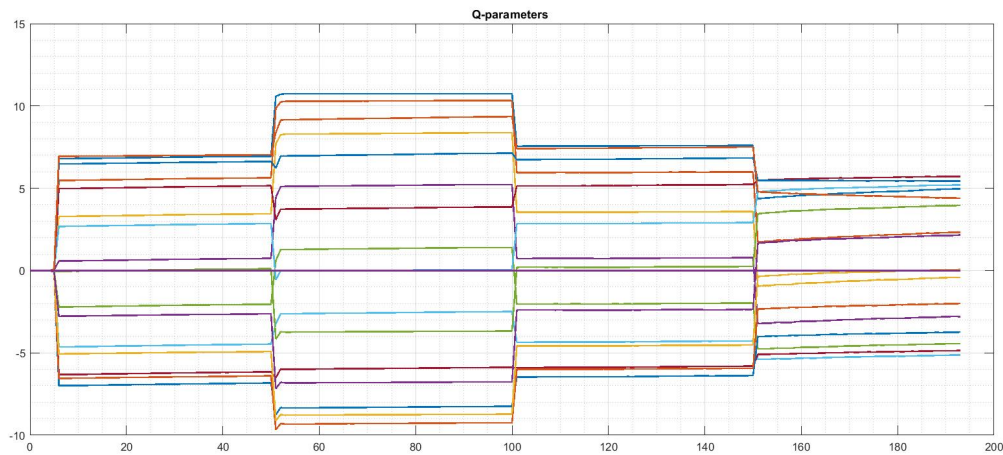


Figure 13: Evolution of the parameters for step changes in the frequency of the disturbance around 160 Hz (16 parameters)

### 6.1.3. The case of 2 sinusoidal disturbances of distinct frequencies

To asymptotically reject the effect of two simultaneous sinusoidal disturbances with distinct frequencies and to assure simultaneously the stability of the system the dimension of the Q filter should be significantly augmented. For  $n_Q = 59$  (60 parameters) it is possible to assure a stable operation of the system for any combination of frequencies in the range 70 Hz to 190 Hz. Fig. 16 gives the time response for a sequence of steps on the frequencies of two sinusoidal disturbances. The initial frequencies of the two sinusoids are 80 Hz and 180 Hz. At  $t = 25$  s one switches to 70 Hz and 170 Hz. At  $t = 50$  s one returns to 80 Hz and 180 Hz and at  $t = 75$ , one switches to 90 Hz and 190 Hz. The corresponding evolution of the parameters is shown in Fig. 17. Table 3 summarizes

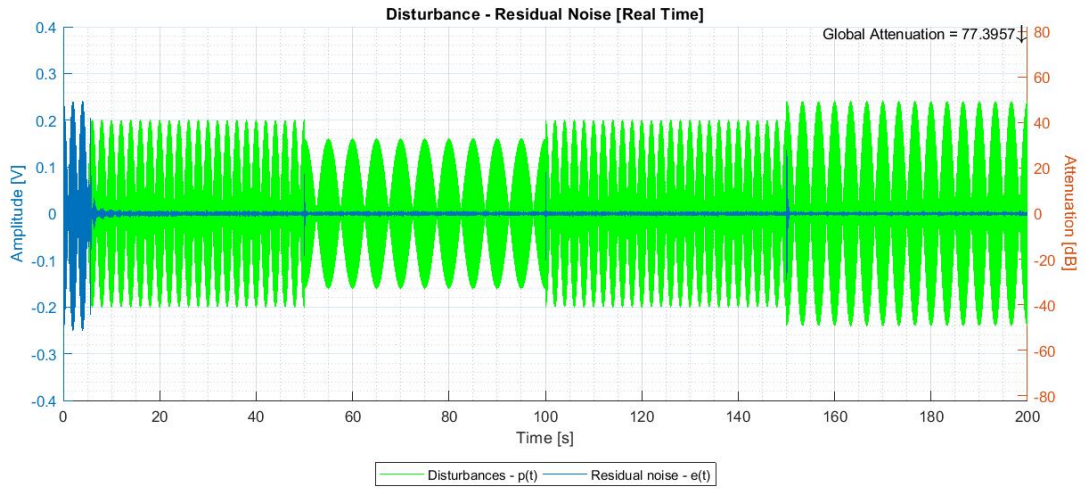


Figure 14: Time response of the residual noise for step changes in the frequencies of an interference phenomenon (16 parameters)

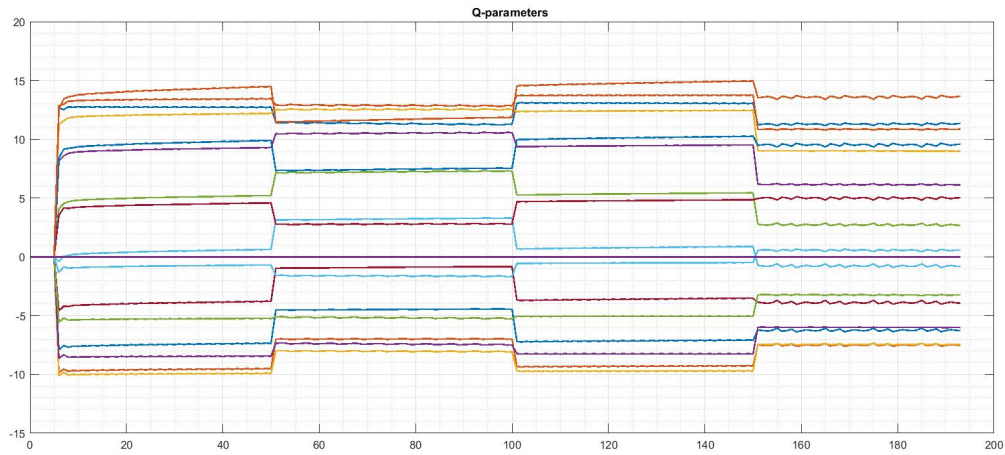


Figure 15: Evolution of the parameters for step changes in the frequencies of an interference phenomenon (16 parameters)

steady states global attenuation results for the case of two simultaneous sinusoidal disturbances with distinct frequencies.

Frequency (Hz)	80/180	90/190	130/170	80/110	80/150	90/120
Model Go, 60 par.(dB)	85.95	90.72	67.04	75.33	72.21	76.02

Table 3: Steady state attenuation for two simultaneous sinusoidal disturbances with distinct frequencies.

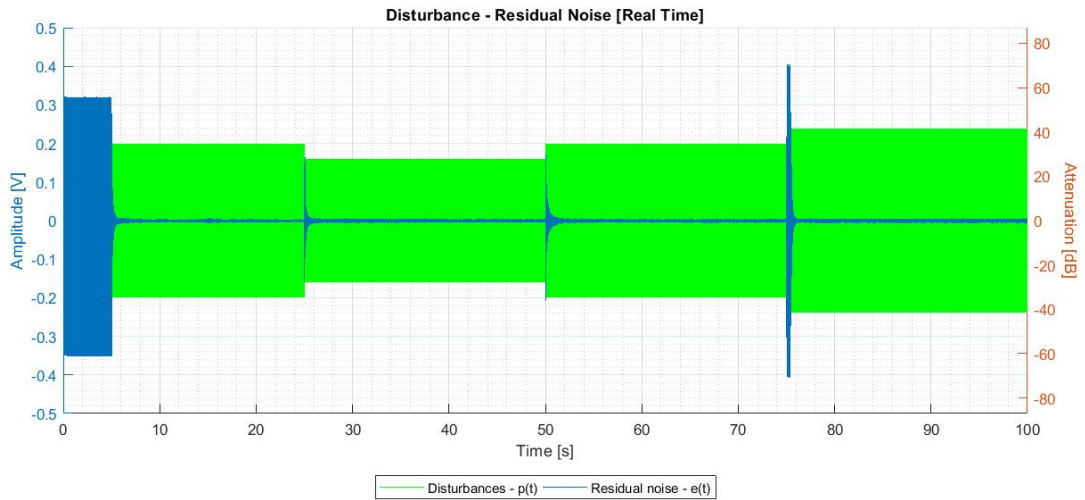


Figure 16: Time response of the residual noise for step changes in the frequency of two simultaneous sinusoidal disturbances around 80 Hz and 180 Hz

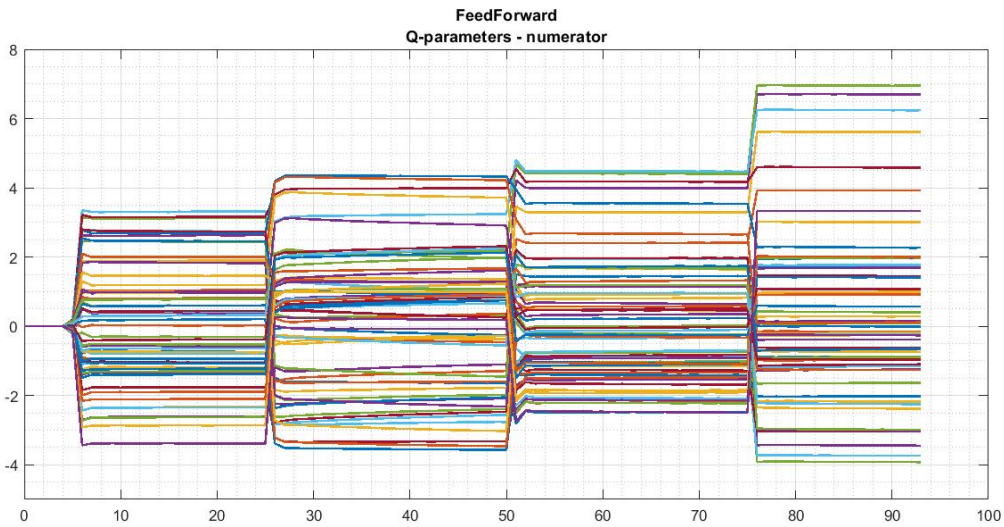


Figure 17: Evolution of the parameters for step changes in the frequency of two simultaneous sinusoidal disturbances around 80 Hz and 180 Hz

#### 6.1.4. Multiplicity of solutions

Since one uses an overparametrized Q filter with respect to the complexity of the model of the disturbance, the solution for the asymptotic rejection of the disturbances is not unique and the values of the Q filter will depend on the initial conditions and previous values of the characteristic of the disturbance. Not all of these solutions assure the stability for the system. Therefore once the parameters go beyond certain limits it is necessary to keep them within these limits as indicated by the theoretical analysis developed in this paper. For specific excitation protocols this phenomenon

is visible. Once this limit is reached the algorithm is re-initialized at 0 for all the parameters (projection to the origin). Fig. 18 shows the evolution of the residual noise for a succession of step frequencies changes for an interference phenomenon around 160 Hz and 160.5 Hz. A cycle of 4 steps changes in frequency of 120 s duration is repeated 10 times over an horizon of 1200 s . The associated evolution of the parameters is shown in Fig. 19. One observes that despite the fact the performances are repetitive, a drift in the parameters of the Q filter occurs. As soon as one of the parameters reaches the value 15 (which was set for illustrating the procedure), all the parameters are reinitialized at 0. This is clearly visible in Fig. 20 which is a zoom on the Fig. 19.

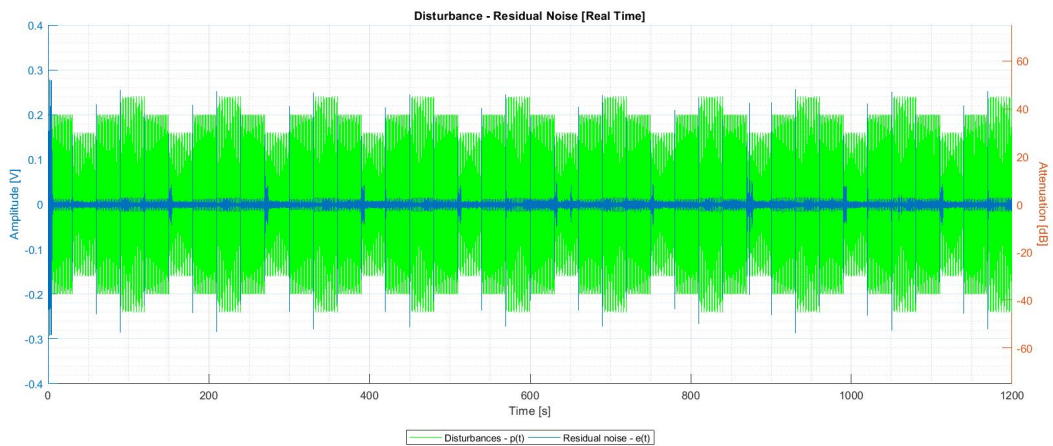


Figure 18: Evolution of the residual noise for step changes in the frequencies of an interference phenomenon over an horizon of 1200s

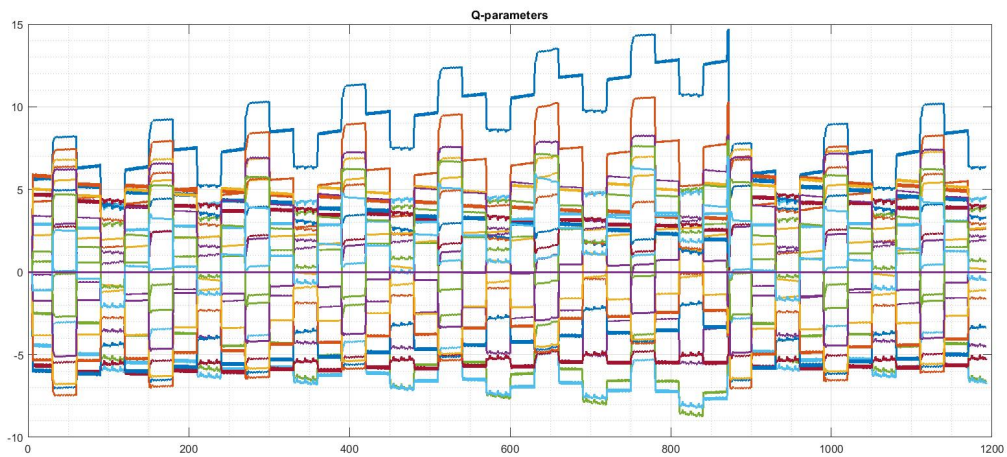


Figure 19: Evolution of the parameters for step changes in in the frequencies of an interference phenomenon over an horizon of 1200s

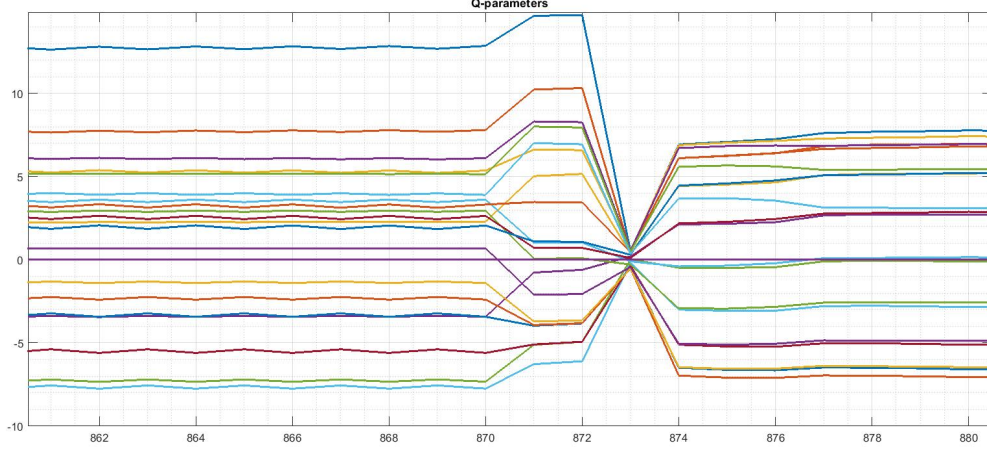


Figure 20: Zoom on the evolution of the parameters at resetting

## 7. Conclusion

The paper has shown that it is possible to handle large uncertainties on the model of the secondary (compensatory) path in adaptive feedback noise attenuation schemes using overparametrization of the compensation filter. However the feasible operation region depends upon a frequency condition related to the discrepancy between the design model and the real model and in addition a linear feedback design has to be done in order to satisfy a frequency condition for stability. Furthermore the standard parameter adaptation algorithm has to be completed with a projection procedure.

### Appendix A. Derivation of Eq. (19)

By combining (5) and (6), one has  $w(t) = -B_0u(t) + A_0 \left( \frac{B}{A}u(t) + d(t) \right) = (-B_0 + A_0 \frac{B}{A})u(t) + A_0d(t)$ , and by including (15) in the previous equation, one obtains  $w(t) = (-B_0 + A_0 \frac{B}{A}) \left( -\frac{H_R}{S_0} Qw(t) \right) + A_0d(t)$ , which yields  $(AS_0 + H_RQ(A_0B - AB_0))w(t) = A_0ASd(t)$ , hence the result.  $\square$

### Appendix B. Derivation of Eq. (20)

By combining (19) and (20) one has  $u(t) = -\frac{H_R}{S_0} Q \frac{AS_0A_0}{AS_0 + QH_R(BA_0 - B_0A)} d(t)$ , thus  $y(t) = \frac{B}{A} - \frac{H_R}{S_0} Q \frac{AS_0A_0}{AS_0 + QH_R(BA_0 - B_0A)} d(t) + d(t)$  which leads to the expression  $y(t) = \frac{(-BH_RQA_0 + AS_0 + H_RQ(A_0B - AB_0))}{AS_0 + H_RQ(A_0B - AB_0)} d(t)$ . By sorting the terms, one gets  $y(t) = \frac{AS_0 - H_RQAB_0}{AS_0 + H_RQ(A_0B - AB_0)} d(t)$ , and the result is obtained.  $\square$

### Appendix C. Derivation of conditions (22) and (23)

According to the expression of the direct sensitivity function (20), the closed-loop is stable if and only if the polynomial  $AS_0 + H_RQ(A_0B - AB_0)$  has all its roots strictly inside the

unit circle. This stability condition is equivalent to the stability condition of the closed loop shown in Fig. C.21). and according to the small gain theorem condition  $b$ ) is obtained. Now

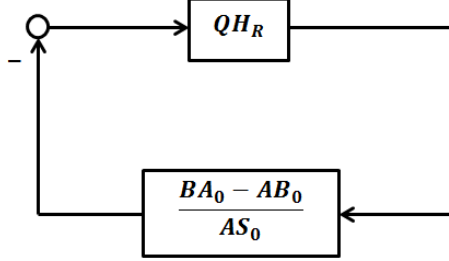


Figure C.21: Equivalent closed-loop

at the frequencies  $\omega_j$  of the disturbance, where  $D(e^{-i\omega_j}) = 0$ , the Bezout equation (13), one has  $H_R(e^{-i\omega_j})B_0(e^{-i\omega_j})Q(e^{-i\omega_j}) = S_0(e^{-i\omega_j})$ , therefore  $Q = \frac{S_0(e^{-i\omega_j})}{H_R(e^{-i\omega_j})B_0(e^{-i\omega_j})}$  and condition  $b$ ) becomes

$$1 < \left| \frac{A(e^{-i\omega_j})B_0(e^{-i\omega_j})}{B(e^{-i\omega_j})A_0(e^{-i\omega_j}) - A(e^{-i\omega_j})B_0(e^{-i\omega_j})} \right|$$

hence condition  $a$ ).  $\square$

#### Appendix D. Stability analysis of the adaptive scheme

The following theorem summarizes the stability analysis of the adaptive scheme

**Theorem 1.** *Under the assumptions:*

- *Plant  $G$  is asymptotically stable.*
- *Disturbance  $d(t)$  has the form (4) and is bounded*
- *It exists  $Q(q^{-1}) \in \mathcal{D}$  with  $n_D - 1 \leq n_Q < \infty$  satisfying (13) and assuring that the polynomial (18) has all its roots strictly inside the unit circle.*

then one has:

$$\lim_{t \rightarrow \infty} v(t+1) = 0 \quad (\text{D.1})$$

and if in addition:

$$\max_{\hat{\theta} \in \mathcal{D}} (\|\hat{Q} - Q\|_1) \left\| \frac{H_R(BA_0 - B_0A)}{AS_0 + QH_R(BA_0 - B_0A)} \right\|_1 < 1 \quad (\text{D.2})$$

one has:

$$w(t), u(t), y(t) \text{ are bounded} \quad (\text{D.3})$$

and:

$$\lim_{t \rightarrow \infty} v^o(t+1) = \lim_{t \rightarrow \infty} y(t+1) = 0 \quad (\text{D.4})$$

Remark : For  $G = G_0$ , the condition (D.2) is automatically satisfied. Similar situation occurs for the case  $n_Q = n_D - 1$  if (18) is satisfied since the persistence of excitation drives  $\tilde{Q}(t) = \hat{Q}(t) - Q$  to zero.

Proof: The equation of the a posteriori adaptation error (32) has the form considered in Theorem 3.2 from [?] (pp 104-105) and since  $H(q^{-1}) = 1$ , one immediately concludes that (D.1) holds. To go further one has to show that  $\mathbf{w}(t)$  and respectively  $w(t)$  are bounded  $\mathbf{w}(t)$  contains delayed and filtered signals generated by  $w(t)$ .

Set  $\Gamma = AS_0$  and  $\bar{\Delta} = H_R(BA_0 - AB_0)$ . In an adaptive context using (19), one can write:

$$(\Gamma + \bar{\Delta}\hat{Q}(t))w(t) = (\Gamma A_o)d(t) \quad (\text{D.5})$$

or alternatively:

$$(\Gamma + \bar{\Delta}\hat{Q}(t) \pm \bar{\Delta}Q)w(t) = (\Gamma A_o)d(t) \quad (\text{D.6})$$

Set  $N = \Gamma A_o$ , and  $\tilde{Q}(t) = \hat{Q}(t) - Q$  and (D.6) can be written as:

$$w(t) = \frac{N}{\Gamma + \bar{\Delta}Q}d(t) - \tilde{Q}(t)\frac{\bar{\Delta}}{\Gamma + \bar{\Delta}Q}w(t) \quad (\text{D.7})$$

which corresponds to a feedback system with an external bounded excitation whose output is  $w(t)$ , shown in Fig. D.22. The input to the equivalent feedback system  $\bar{d} = \frac{N}{\Gamma + \bar{\Delta}Q}d(t)$  has the property:

$$\|\bar{d}(t)\|_\infty \leq \left\| \frac{N}{\Gamma + \bar{\Delta}Q} \right\|_1 d_m(t) \quad (\text{D.8})$$

where  $d_m(t) = \sup|d(t)| = \|d(t)\|_\infty$  and  $\left\| \frac{N}{\Gamma + \bar{\Delta}Q} \right\|_1$  is finite. The output of the feedback path  $x(t)$  is given by

$$x(t) = \frac{\bar{\Delta}\tilde{Q}}{\Gamma + \bar{\Delta}Q}w(t) \quad (\text{D.9})$$

and therefore:

$$\|w(t)\|_\infty \leq \|\bar{d}(t)\|_\infty + \|\tilde{Q}\|_1 \left\| \frac{\bar{\Delta}}{\Gamma + \bar{\Delta}Q} \right\|_1 \|w(t)\|_\infty \quad (\text{D.10})$$

Applying small gain arguments [?] and taking into account that the equivalent feedforward path has unitary gain one concludes that condition (D.2) assures the boundedness of  $w(t)$ . From the definition of  $\mathbf{r}(t)$  given in (29), one concludes also that  $\mathbf{w}(t)$  is bounded and taking in account (34) one concludes that (D.4) is true. Since  $y(t)$  is bounded in finite time (and goes to zero),  $w(t)$  is bounded and  $Q$  is bounded one concludes that  $u(t)$  is also bounded.  $\square$

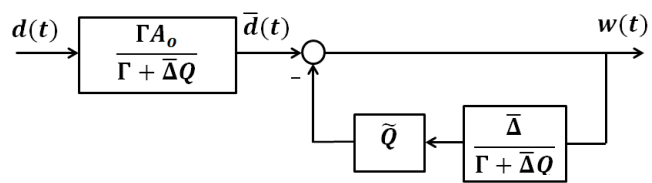


Figure D.22: Generation of  $w(t)$ .